DE GRUYTER OPEN

Chemical and Process Engineering 2017, 38 (2), 307-319
DOI: 10.1515/cpe-2017-0024

PAN

EXTERNAL MASS TRANSFER MODEL FOR HYDROGEN PEROXIDE DECOMPOSITION BY TERMINOX ULTRA CATALASE IN A PACKED-BED REACTOR

Ireneusz Grubecki*

UTP University of Science and Technology, Faculty of Chemical Technology and Engineering,
3 Seminaryjna Street, 85-326 Bydgoszcz, Poland

It is known that external diffusional resistances are significant in immobilized enzyme packed-bed reactors, especially at large scales. Thus, the external mass transfer effects were analyzed for hydrogen peroxide decomposition by immobilized Terminox Ultra catalase in a packed-bed bioreactor. For this purpose the apparent reaction rate constants, k_P, were determined by conducting experimental works at different superficial velocities, U, and temperatures. To develop an external mass transfer model the correlation between the Colburn factor, J_D, and the Reynolds number, Re, of the type $J_D = K\,Re^{(n-1)}$ was assessed and related to the mass transfer coefficient, k_{mL}. The values of K and n were calculated from the dependence $(a_m k_p^{-1} - k_R^{-1})$ vs. Re^{-1} making use of the intrinsic reaction rate constants, k_R, determined before. Based on statistical analysis it was found that the mass transfer correlation $J_D = 0.972\,Re^{-0.368}$ predicts experimental data accurately. The proposed model would be useful for the design and optimization of industrial-scale reactors.

Keywords: hydrogen peroxide decomposition, immobilized terminox ultra catalase, packed bed reactor, external film diffusion, mass transfer coefficient

1. INTRODUCTION

Catalases (EC 1.11.1.6) are abundant enzymes in nature that decompose hydrogen peroxide to water and molecular oxygen (Zámocký and Koller, 1999). These enzymes can find many industrial applications, namely: 1) in the textile industry after textile blenching (Costa et al., 2002a), 2) in the food industry after cold pasteurization of milk (Farkye, 2004), 3) coupled with oxidases, prevention of the inactivation of the oxidases by the deleterious action of a high concentration of peroxide (Fernández-Lafuente et al., 1998) and 4) coupled with oxidases, prevention of side reactions caused by the H_2O_2 that can destroy the target product (Schoevaart and Kieboom, 2001). It is worth noting that application of catalase reduces 48% of the energy consumption, 83% of the chemical costs, 50% of the water consumption and 33% of the processing time (Eberhardt et al., 2004). However, direct application of free catalase promotes interaction between the protein and the dye which in turn reduces dye uptake by the fabric. Immobilization of catalase overcomes this constraint and concomitantly enables reuse of the enzyme. The attempts of catalase immobilization have been made by several authors by using organic and inorganic materials (Alptekin et al., 2011; Betancor et al., 2003; Vera-Avila et al., 2004;). However, when working with immobilized enzymes mass-transfer resistances are likely to occur no matter which method of immobilization is used. Two types of resistances may occur (Illanes et al., 2014): 1) external diffusional resistances (EDR) when the rate of diffusional transport through the stagnant layer surrounding the solid biocatalyst particle is the limiting one, 2) internal diffusional resistances (IDR) when the substrate will have to diffuse from the biocatalyst

*Corresponding authors, e-mail: ireneusz.grubecki@utp.edu.pl

surface inside the biocatalyst internal structure at the diffusion rate lower than that in the bulk liquid phase. Usually penetration of the substrate into the interior of the biocatalyst particle is the slowest step. Hence, the EDR are negligible compared to IDR. In many cases this assumption is often but not always valid. So, in the case of significant EDR the combined effect of EDR and IDR is described (Mudliar et al., 2008). The analysis of a combined effect of EDR and IDR can also be indicated in the case of hydrogen peroxide decomposition (HPD) by catalase (Traher and Kittrell, 1974; Greenfield et al., 1975). Hence, the reports on immobilized enzyme (especially catalase) dealing only with EDR effect are limited. In order to analyse EDR the internal diffusional resistances should be eliminated. Thus, in this paper a realistic engineering analysis of the external mass transfer combined with the reaction of the HPD by commercial Terminox Ultra catalase (TUC) immobilized on non-porous glass and correlation of experiment with theory has been carried out. Consequently, an external film diffusion model was developed to predict the behavior of the fixed-bed reactor for enzymatic decomposition of hydrogen peroxide occurring under diffusional resistances. Although film diffusion studies of immobilized catalase in a tubular reactor were taken into account by Greenfield et al. (1975) as well as Traher and Kittrell (1974) it is necessary to evaluate each immobilized enzyme system individually.

2. DEVELOPMENT OF EXTERNAL MASS TRANSFER MODEL

2.1. Apparent reaction rate

External mass transfer analysis presented in this work is developed based on the approach used by Rovito and Kittrell (1973). Thus, in a packed-bed column with ideal plug flow of hydrogen peroxide solution a single biochemical reaction takes place. Taking additionally into account that catalase deactivation is very slow or does not proceed at all, mass balance of the process can be described by the following equation

$$\left(\frac{HQ}{W}\right)\frac{dC_A}{dh} = -r_A \tag{1}$$

The process of HPD by the catalase in industrial practice undergoes at low substrate concentrations (Costa et al., 2002b; Deluca et al., 1995; Tarhan and Telefoncu, 1990; Tarhan and Uslan, 1990; Tarhan, 1995; Vasudevan and Weiland, 1990; Vasudeven and Weiland, 1993). Thus, a relationship between the reaction rate, r_A, and the substrate (hydrogen peroxide) concentration in the bioreactor (at the fixed activity of catalase) is given by

$$r_A = k_P C_A \tag{2}$$

Substitution of Eq. (2) into Eq. (1) and integration of the resulting equation subject to the boundary conditions given below

$$C_A(h=0) = C_{A,In} \tag{3a}$$

$$C_A(h=H) = C_{A,Out} \tag{3b}$$

yields

$$ln\left(\frac{1}{1-\alpha}\right) = k_P\left(\frac{W}{Q}\right) \tag{4}$$

The apparent reaction rate constant, k_P, can be found from Eq. (4) based on the experimentally measured conversion values, α, assessed at different volumetric flow rates, Q, and quantities of immobilized catalase, W.

2.2. Combined mass transfer and reaction of hydrogen peroxide decomposition

The mass transport rate of the H_2O_2 from the bulk liquid to the outer surface of the immobilized beads is proportional to the external mass transfer coefficient, k_{mL}, area of the external mass transfer, a_m, and the H_2O_2 concentration difference between the bulk, C_A, and the external surface of immobilized beads, C_{As}:

$$r_m = k_{mL} a_m (C_A - C_{As}) \tag{5}$$

The surface area per unit of weight, a_m, can be determined as

$$a_m = \frac{6(1-\varepsilon)}{d_P \rho_U} \tag{6}$$

The rate of hydrogen peroxide decomposition can be expressed by Eq. (7)

$$r_A = k_R a_m C_{As} \tag{7}$$

At a steady state process, the rate of mass transfer, r_m, is equal to the reaction rate, r_A. Thus, equating Eq. (5) with Eq. (7) and solving for the unknown surface concentration of hydrogen peroxide, Eq. (8) is obtained

$$C_{As} = \frac{k_{mL}}{k_{mL} + k_R} C_A \tag{8}$$

Equation (8) represents the H_2O_2 behaviour under EDR. A combination of Eqs. (2), (7) and (8) leads to a dependence between the pseudo first-order, k_P, and intrinsic, k_R, reaction rate constants as well as the mass transfer coefficient, k_{mL}

$$k_P = \frac{k_{mL} k_R a_m}{k_{mL} + k_R} \tag{9}$$

2.3. External mass transfer correlation model

It is known that external mass transfer coefficient, k_{mL}, changes with many parameters (Kalaga et al., 2014). Therefore, a correlation allowing to determine a mass transfer coefficient at different operating parameters is needed. Such a correlation may be obtained by defining a dimensionless group:

$$J_D = \mathrm{St}_D \mathrm{Sc}^{2/3} \tag{10}$$

A large number of correlations describing J_D - factor as a function of Reynolds number (Re) are available as follows (Dizge and Tansel, 2010)

$$J_D = K \,\mathrm{Re}^{(n-1)} \tag{11}$$

Different values of K and n are related to different mass transfer conditions. The value of n varies from 0.1 to 1.0 depending on the flow characteristics. Equating Eq. (10) with Eq. (11) yields a dependence for the external mass transfer coefficient

$$k_{mL} = A G^n \tag{12}$$

$$A = \frac{K}{\rho} \mathrm{Sc}^{-2/3} \left(\frac{d_P}{\eta} \right)^{n-1} \tag{13}$$

Substituting Eq. (12) in Eq. (9) leads to the following correlation

$$\frac{1}{k_P} = \frac{1}{Aa_m}\left(\frac{1}{G^n}\right) + \left(\frac{1}{k_R a_m}\right) \tag{14}$$

The experimentally measured values of k_P^{-1} vs.G^{-n} for various values of K and n can be plotted. From a straight line with a slope, $(Aa_m)^{-1}$, and an intercept, $(k_R a_m)^{-1}$, a_m and k_R values can then be determined. The estimated values of a_m are compared to that calculated from Eq. (6) to determine the set of K and n values adequate for HPD in the packed-bed.

A trial-and-error procedure can be neglected, when a value of the reaction rate constant (k_R) is known and assessed independently. In such a case Eq. (14) can be expressed by

$$Y = \left(\frac{1}{Re}\right)^n \times \left[K^{-1} Sc^{2/3}\left(\frac{\rho d_P}{\eta}\right)\right] \tag{15}$$

where $Y = a_m k_P^{-1} - k_R^{-1}$. From Eq. (15) the slope of the $\ln(Y)$ - $\ln(\mathrm{Re}^{-1})$ plot should correspond to n and its intercept $\ln[K^{-1}\mathrm{Sc}^{2/3}(\rho d_P \eta^{-1})]$.

3. MATERIALS AND EXPERIMENTAL PROCEDURE

3.1. Preparation of immobilized catalase beads

Terminox Ultra catalase (E.C. 1.11.1.6; 50,000 U/g) was immobilized by glutaraldehyde-coupling to the silanised support according to the method of Vasudevan and Weiland (1990). In order to eliminate any IDR, non-porous glass beads (425-600 μm) were used as a support. Commercial TUC was purchased from Novozymes (Bagsvaerd, Denmark), (gamma-aminopropyl)triethoxysilane as well as glutaraldehyde (50% w/w aqueous solution) were purchased from Sigma-Aldrich (Steinheim, Germany). All other chemicals employed, including commercial hydrogen peroxide (30% w/w aqueous solution), were products of Avantor Performance Materials (Gliwice, Poland).

3.2. Packed bed enzyme reactor studies

The experimental set-up used in this study consisted of a vertical tubular reactor, peristaltic pump, flowmeter and feed solution container (Fig. 1). The test tubular reactor ($8 \cdot 10^{-3}$ m inner diameter and height adjusted to the bulk mass of the biocatalyst) was jacketed and water from a thermostat was circulated through the jacket. The feed flow rate of the H_2O_2 solution (concentration of about $85 \cdot 10^{-3}$ kg·m^{-3}) was forced through the packed-bed reactor by a peristaltic pump and controlled by a flowmeter.

At both ends the reactor was equipped with a screen made of stainless steel. A biocatalyst bed was set on the bottom screen while the upper screen served to prevent biocatalyst entrainment by the outflowing substrate stream. The experiments were conducted in two steps. In the first one the values of pseudo first-order rate constant, k_P, were obtained (Eq. (4)) by collecting samples at the various bed mass (from $0.5 \cdot 10^{-3}$ kg to $3.5 \cdot 10^{-3}$ kg) under different superficial velocities (from $4.0 \cdot 10^{-3}$ m·s^{-1} to $10.3 \cdot 10^{-3}$ m·s^{-1}). In each case, the plug flow condition with no axial dispersion has been satisfied (Burghardt and Bartelmus, 2001).

In the second step the intrinsic rate constants for reaction, k_R, and (at the same time) for deactivation, k_D, were determined. These kinetic parameters of the immobilized TUC represent its proper behaviour and correspond to that observed in the absence of EDR.

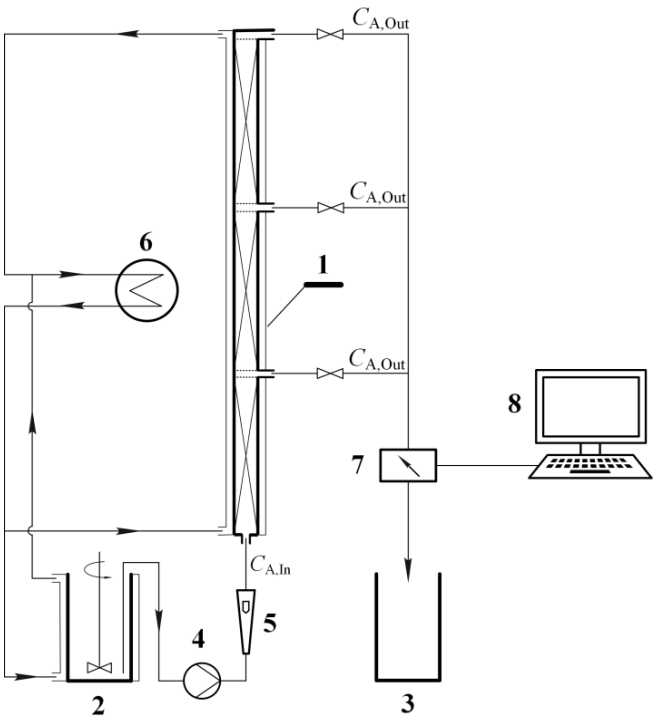

Fig. 1. Experimental set-up: 1-tubular bioreactor, 2-feed solution tank, 3-product collector, 4-peristaltic pump, 5-flowmeter, 6-thermostat, 7-spectrophotometer, 8-computer

Such conditions (feed flow rate) have been established by monitoring the H_2O_2 concentration in the outlet stream under the various superficial velocities and invariable residence time. Then, the conversion measurements were done (Altomare et al., 1974). It was accomplished by combining three reactors in series and filling each of them with biocatalyst of a mass of $11 \cdot 10^{-3}$ kg established earlier. The bulk density of biocatalyst bed equaled to 1823 kg·m^{-3} (bed porosity of $\varepsilon = 0.3$) corresponded to the bed depth of ca. 0.12 m in each segment. Such a system of three combined reactors may be considered as a single reactor enabling to control H_2O_2 conversion, α, as a function of time, t ($\tau = tQ\rho_U / W$), and position, h ($z = h / H$). From measurements a discrete function

$$\alpha(z_i, \tau_j) = 1 - C_{A,Out}(z_i, \tau_j) / C_{A,In} \quad (i = 1...M,\ j = 1...N) \tag{16}$$

was formulated.

The experimental data described by Eq. (16) were fitted to an equation derived by Altomare et al. (1974)

$$\alpha(z_i, \tau_j) = 1 - \frac{\exp[\beta_2(\tau_j - z_i)]}{\exp(\beta_1 z_i) + \exp[\beta_2(\tau_j - z_i)] - 1} \tag{17}$$

using a non-linear least squared regression method which minimizes the sum of deviation squares in a series of iterative steps. In Eq. (17) β_1 and β_2 can be expressed as

$$\beta_1 = \frac{W}{Q} k_R a_m \tag{18}$$

$$\beta_2 = \frac{W}{Q\rho_U} k_D C_{A,In} \tag{19}$$

The experiments were conducted at a superficial velocity of U =$5 \cdot 10^{-2}$ m·s^{-1} and repeated for temperature values ranging from 278K to 323K.

3.3. Analysis of hydrogen peroxide concentration

The concentration of H_2O_2 in the exit stream of reactor was monitored spectrophotometrically making use of a UV-Vis Jasco V-530 spectrophotometer (Artisan T.G., Champaign IL, USA) equipped with a quartz cuvette Q11020 (Gallab, Warsaw, Poland) with optical light path of 20 mm. The measurements were carried out at 240 nm ($\varepsilon_{240} = 39.4$ dm^3·mol^{-1}·cm^{-1}).

4. RESULTS AND DISCUSSION

4.1. Determination of the specific surface area for the mass transfer

In order to estimate a value of the mass transfer interfacial area information on the diameter of a single bed element is indispensable. It was assessed on the basis of a sieve analysis carried out using the Vibratory Sieve Shaker Analysette 3 Pro system (Fritsch GmbH, Germany). In consequence, an average particle diameter of $d_P = 5.05 \cdot 10^{-4}$ m was determined. Now, making use of Eq. (6) it is possible to calculate the specific external surface area of the biocatalyst equal to $a_m = 4.57$ m^2·kg^{-1}.

4.2. Determination of intrinsic kinetic parameters

A function, $\alpha = \alpha(z_i, \tau_j)$ describing a relationship between conversion of H_2O_2 and position in the reactor, z, and time, τ, (Eq. (17)) was fitted to the experimental data (Eq. (16)) using a non-linear least squares regression procedure with Matlab Optimization Toolbox (Mathworks Inc., Natick MA, USA). As a result, values of intrinsic rate constants for reaction, k_R, and deactivation, k_D, were obtained (Fig. 2). Based on these values the activation energy for reaction and the frequency factor in the Arrhenius equation equal to $E_R = 12.57 \pm 0.30$ kJ·mol^{-1} and $k_{R0}a_m = (26.32 \pm 2.95) \cdot 10^{-3}$ m^3·kg^{-1}·s^{-1}, respectively, were assessed.

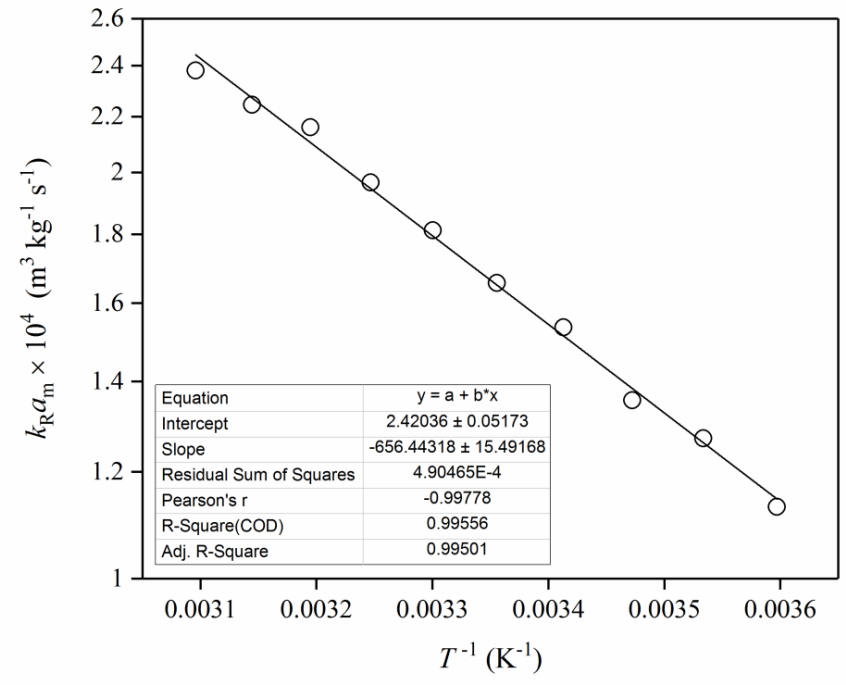

Fig. 2. Dependence of $k_R a_m$ vs. (T^{-1}) for HPD and $C_{A,In} = 85 \cdot 10^{-3}$ kg·m^{-3}

These values were used at formulation of the external mass transfer model. The kinetic parameters for deactivation of immobilized catalase were also determined but in the present analysis have been neglected.

4.3. External mass transfer model

Measurements of pseudo first-order reaction rate constants, k_P, were carried out under the process conditions for which the rate of TUC deactivation can be negligible. Such conditions correspond to low values of H_2O_2 concentration, $C_{A,In} = 85 \cdot 10^{-3}$ kg·m^{-3}, temperature in the range from 278K to 303K and $pH = 7$ (Cantemir et al., 2013). The results of these measurements are plotted in Fig. 3 in a form of a dependence $k_P = k_P(U,T)$.

It can be seen that with an increasing superficial velocity, U, values of the pseudo first-order rate constant, k_P, increase. For example, the increase of U from $4 \cdot 10^{-3}$ m·s^{-1} to $10.3 \cdot 10^{-3}$ m·s^{-1} resulted in an increase of k_P from $4.82 \cdot 10^{-5}$ m^3·kg^{-1}·s^{-1} to $6.50 \cdot 10^{-5}$ m^3·kg^{-1}·s^{-1} at $T = 278$ K and from $8.68 \cdot 10^{-5}$ m^3·kg^{-1}·s^{-1} to $11.47 \cdot 10^{-5}$ m^3·kg^{-1}·s^{-1} at $T = 303$ K. For investigation of the film diffusion effects on the HPD rate the Reynolds numbers and superficial mass velocities at the studied feed flow rates were also calculated (Table 1). Due to relatively low concentrations of H_2O_2 in the solution its density and dynamic viscosity were assumed as those for water. Only diffusivity equal to $D_f = 8.80 \cdot 10^{-10}$ m^2·s^{-1} was taken based on the data of USP Technologies Company (2017) at 293K. For others temperatures, diffusivities were calculated according to the Stokes-Einstein equation (Curcio et al., 2015).

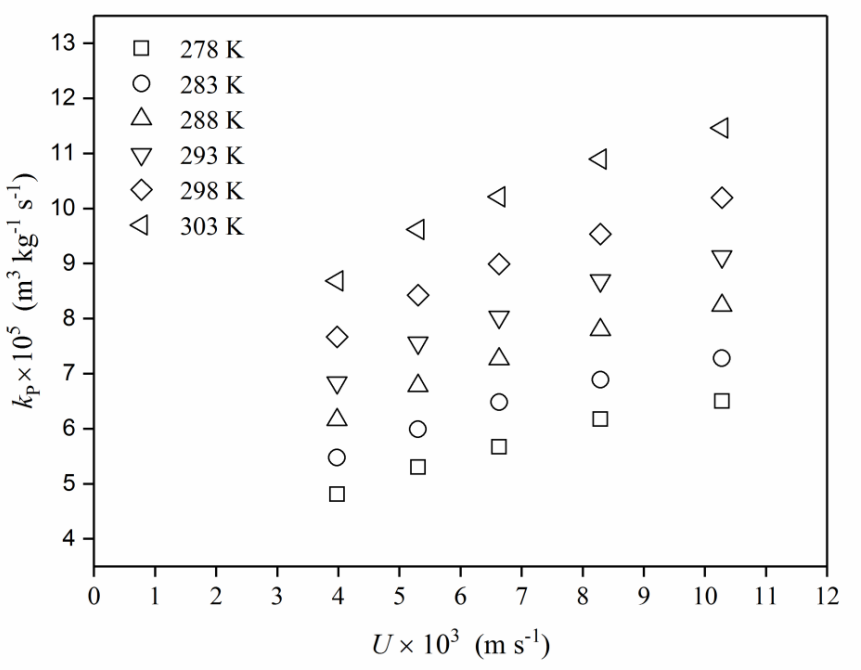

Fig. 3. Dependence of k_P vs. U for various temperatures

Having established values of the pseudo first-order rate constants, k_P, and the Reynolds numbers it is now possible to determine the values of n and K (Eq. (11)) using Eq. (15). At a fixed temperature (in a log-log plot) this equation yields a straight line with slope n and intercept $\ln[K^{-1}\mathrm{Sc}^{2/3}(\rho d_P \eta^{-1})]$. Thus, Eq. (15) was fitted to the experimental data using coordinates $(a_m k_P^{-1} - k_R^{-1})$ vs. (Re^{-1}) and non-linear least squares regression procedure with Matlab Optimization Toolbox (Mathworks Inc., Natick MA, USA) which minimizes the sum of deviation squares for all analyzed temperature values (Fig. 4). In this way the following values were obtained $n = 0.632 \pm 0.001$ and $K = 0.972 \pm 0.001$ while the

calculated values of the regression coefficient, $R^2 = 0.9986$, as well as the sum of squared error (SSE), and the root mean squared error (RMSE) were equal to SSE = $6.300 \cdot 10^{-4}$ s·m^{-1} and RMSE = $4.743 \cdot 10^{-3}$ s$^{0.5}$·m$^{-0.5}$, respectively, confirming that the developed model offers a quite good fit to the experimental data based on previously determined values of the pseudo first-order rate constants data. This conclusion is also confirmed by the statistical parameters estimated when the dependent variables, $Y = a_m k_P^{-1} - k_R^{-1}$, and, k_P^{-1}, determined experimentally have been compared with those calculated from Eqs. (15) and (14), for $n = 0.632$ and $K = 0.972$, respectively (Tables 2 and 3).

Table 1. The values of Reynolds number, Re, and superficial mass velocity, G, at studied feed flow rates, Q, and temperatures, T

$Q \cdot 10^7$ m^3·s^{-1}	$U \cdot 10^3$ m·s^{-1}	G kg·m^{-2}·s^{-1}	Re_{278}	Re_{283}	Re_{288}	Re_{293}	Re_{298}	Re_{303}
2.00	4.00	4.00	1.34	1.54	1.76	2.00	2.25	2.52
2.67	5.31	5.30	1.78	2.05	2.34	2.66	3.00	3.36
3.33	6.63	6.63	2.23	2.56	2.93	3.33	3.75	4.19
4.17	8.29	8.29	2.78	3.20	3.66	4.16	4.69	5.24
5.17	10.28	10.28	3.45	3.97	4.54	5.16	5.82	6.50

Re_T denotes the value of Reynolds number at temperature T (K)

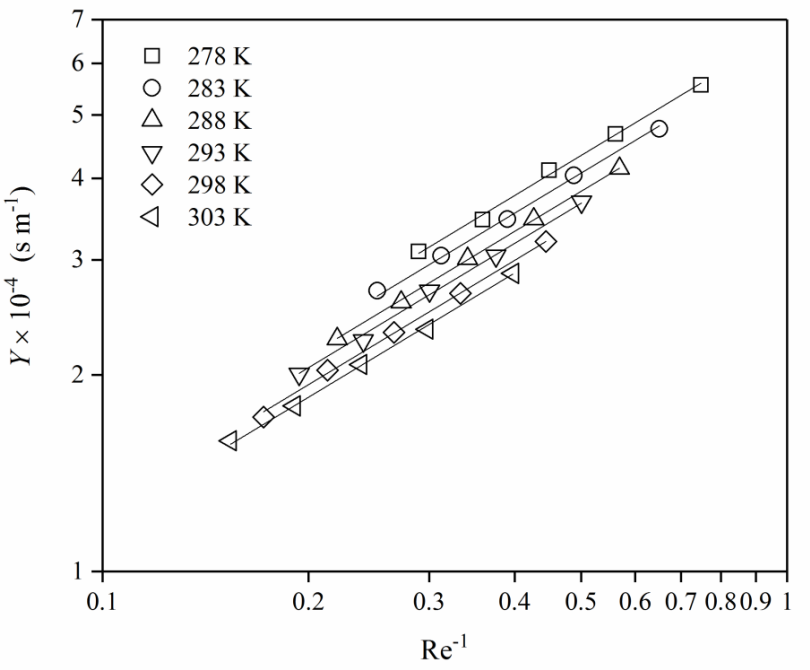

Fig. 4. Dependence of Y vs. Re^{-1} for different temperature values

It should be noticed that the relative percentage deviations of a_m and $k_R a_m$ calculated from Eq. (14) (Table 3) compared with the experimental values of $a_m = 4.57$ m^2·kg^{-1} and $k_R\, a_m$ did not exceed 3.72% and 4.94%, respectively. After accomplishing statistical analysis of n and K it is possible to obtain the variations of mass transfer coefficient, k_{mL}, with G or Re (Table 1) from Eq. (9). These results are illustrated in Fig. 5. From Eq. (12) n and K values were assessed again to be equal to $n = 0.632 \pm 0.007$ and $K = 0.972 \pm 0.022$ with determination coefficient of $R^2 = 0.9984$ as well as the sum of squared error (SSE) and the root mean squared error (RMSE) equal to SSE = $3.991 \cdot 10^{-4}$ m·s^{-1} and RMSE = $3.776 \cdot 10^{-3}$ m$^{0.5}$ s$^{-0.5}$, respectively. They confirm that the present mathematical analysis is self-consistent.

Table 2. The comparison of the values Y obtained from experimental data with those calculated from Eq. (15) for $n = 0.632$ and $K = 0.972$

T K	R^2	SSE $\cdot 10^4$ $s \cdot m^{-1}$	RMSE $\cdot 10^3$ $s^{0.5} \cdot m^{-0.5}$
278	0.9975	1.313	6.615
283	0.9975	1.105	6.068
288	0.9996	0.833	5.271
293	0.9976	1.327	6.652
298	0.9988	1.045	5.902
303	0.9986	0.676	4.748

Table 3. Statistical parameters of estimates for Eq. (14) at various temperatures

i	T K	$A \cdot 10^5$ $kg^{-0.632} \cdot m^{2.264} \cdot s^{-0.368}$	a_m, $m^2\ kg^{-1}$	$k_R a_m \cdot 10^4$ $m^3\ kg^{-1}\ s^{-1}$	R^2	SSE $\cdot 10^{-4}$ kg s m^{-3}	RMSE $\cdot 10^{-2}$ $kg^{0.5}\ s^{0.5}\ m^{-1.5}$
1	278	0.750	4.60 ± 0.38	1.148 ± 0.122	0.9976	4.418	1.213
2	283	0.869	4.74 ± 0.27	1.228 ± 0.067	0.9995	1.386	0.680
3	288	1.002	4.58 ± 0.16	1.402 ± 0.043	0.9980	0.326	0.330
4	293	1.147	4.46 ± 0.40	1.551 ± 0.114	0.9974	1.660	0.744
5	298	1.304	4.54 ± 0.30	1.671 ± 0.087	0.9989	0.688	0.479
6	303	1.471	4.62 ± 0.31	1.881 ± 0.092	0.9984	0.559	0.432

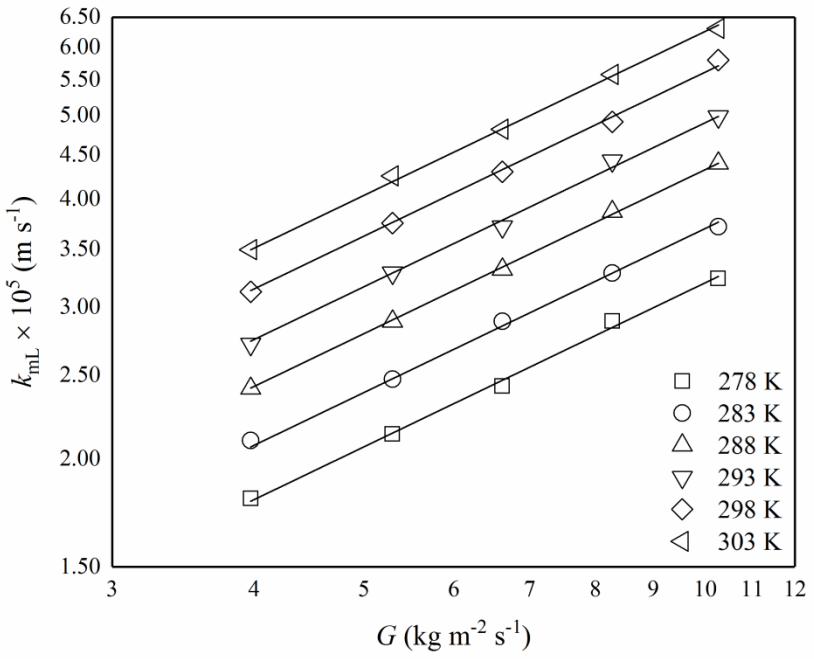

Fig. 5. Dependence of calculated values of the mass transfer coefficient, k_{mL}, on superficial mass velocity, G, for different temperatures

In view of above presented results it can be stated that the external mass transfer correlation of the form

$$J_D = 0.972\,\mathrm{Re}^{-0.378} \tag{20}$$

predicts the experimental data for hydrogen peroxide decomposition by Terminox Ultra catalase in a packed-bed reactor with the normalized deviation lower than 3.6 % (Fig. 6). It should be mentioned that mass transfer coefficients calculated with Eq. (20) are lower by about 30% than those obtained from external mass transfer model developed by Traher and Kittrell (1974) for beef liver catalase. Thus, the external mass transfer model developed in this work (Eq. (20)) may be useful in the process of hydrogen peroxide decomposition by catalase originating from various sources.

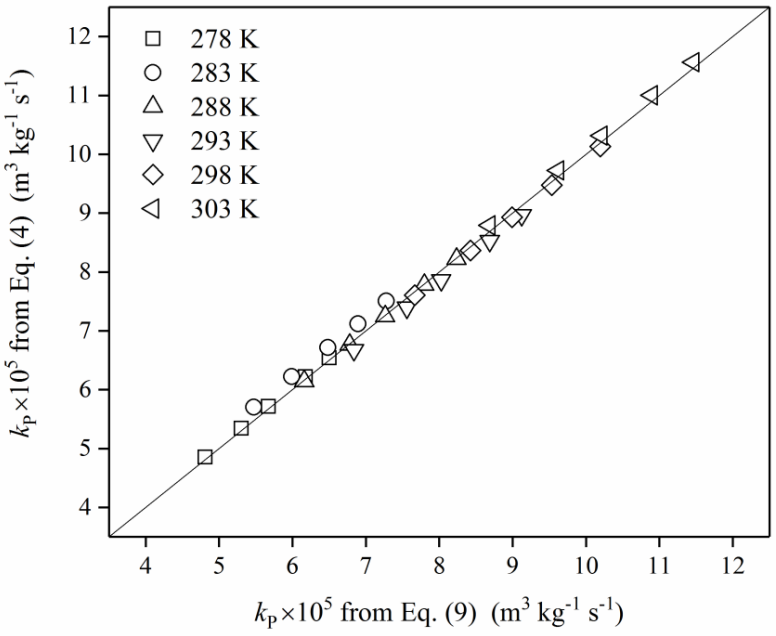

Fig. 6. The comparison of the observed first-order HPD rate constant, k_P, calculated from Eq. (4) with those calculated from Eq. (9) found for all superficial velocities, U, and temperature values

Table 4. Effects of external mass transfer, $k_{mL}a_m$, and intrinsic reaction rate, $k_R a_m$, on pseudo first-order reaction rate, k_P, for selected temperatures.

T, K	$U \cdot 10^3$ m·s^{-1}	$(k_P \cdot 10^3)^{-1}$ kg·s·m^{-3}	$(k_R a_m \cdot 10^3)^{-1}$ kg·s·m^{-3}	% Contribution of $k_R a_m$	$(k_{mL} a_m)^{-1}$ kg·s·m^{-3}	% Contribution of $k_{mL} a_m$
278	4.00	20.78	8.71	41.92	12.07	58.08
	5.31	18.86		46.18	10.15	53.82
	6.63	17.63		49.40	8.92	50.60
	8.29	16.19		53.80	7.48	46.20
	10.28	15.38		56.63	6.67	43.37
298	4.00	13.02	5.99	46.01	7.03	53.99
	5.31	11.88		50.42	5.89	49.58
	6.63	11.10		53.96	5.11	46.04
	8.29	10.50		57.05	4.51	42.95
	10.28	9.78		61.25	3.79	38.75

The combined effects of the intrinsic reaction rate constants, $k_R a_m$, and the mass transfer coefficients, $k_{mL}a_m$, on the apparent reaction rate constants, k_P, for $n = 0.632$ and $K = 0.972$ are compared in Table 4. It can be seen that the apparent reaction rate is affected by both the external film diffusion of H_2O_2 and the biochemical reaction rate. Both steps have significant contributions. At a low superficial velocity ($U = 4.0 \cdot 10^{-3}$ m·s^{-1}) and 278 K the external mass transfer dominates with contribution of 58%. At higher values of U the contribution of mass transfer decreases while the contribution of the reaction rate rises.

For example, at a superficial velocity of $U = 10.3 \cdot 10^{-3}$ m s^{-1} the external mass transfer and biochemical reaction rate contribute with 43.4% and 56.6%, respectively. Additionally, temperature increase makes the biochemical reaction rate contribution larger. Namely, temperature increase from 278 K to 298 K results in the contribution increase of reaction rate from 41.9% to 46.0% for $U = 4.0 \cdot 10^{-3}$ m s^{-1} and from 56.6% to 61.3% for $Q = 10.3 \cdot 10^{-3}$ m s^{-1}.

5. CONCLUSIONS

Based on the results of this study the following conclusions can be drawn:

- The observed apparent reaction rate constant, k_P, increases when the superficial velocity, U, of the hydrogen peroxide solution and temperature increase. This is due to reduction in the film thickness at high superficial velocities and also temperature effects on kinetics of the enzyme catalysed reaction.
- Both external film diffusion, $k_{mL}a_m$, and overall hydrogen peroxide decomposition rate, $k_R a_m$, influence the apparent reaction rate constant, k_P. However, the effects of film diffusion are significant at low superficial velocities as well as low temperatures and should not be ignored when a proper behaviour of immobilized Terminox Ultra catalase under EDR is evaluated.
- The external mass transfer model $J_D = 0.972 \mathrm{Re}^{-0.378}$ offers quite good fit to the experimental data of the pseudo first-order rate constants. This model is valid for low Reynolds numbers in the range of 0.17 - 10. It can be used to quantify the external film diffusion effects for H_2O_2 decomposed by Terminox Ultra catalase in a fixed-bed reactor.
- The approach demonstrated in this work allows to predict the effect of external film diffusion on the observed reaction rates in any operational conditions and will be useful for simulation and optimization of hydrogen peroxide decomposition process in the presence of immobilized Terminox Ultra catalase.

SYMBOLS

A	constant defined by Eq. (13), m^{2n+1} s^{n-1}/kg^n
a_m	surface area per unit weight, m^2/kg
C_A	bulk stream substrate concentration, kg/m^3
C_{As}	surface concentration of hydrogen peroxide, kg/m^3
dC_A/dh	the H_2O_2 concentration gradient along the reactor length, kg/(m^3·m)
D_f	hydrogen peroxide diffusion coefficient, m^2/s
d_P	biocatalyst particle diameter, m
G	superficial mass velocity related to the superficial velocity averaged over the entire cross section of the bed, kg/(m^2·s)
H	bed depth, m
h	distance from reactor inlet, m

z	dimensionless axial distance along the bioreactor ($=h/H$)
J_D	Colburn factor defined by Eq. (10)
K	constant in Eq. (11) related to different mass transfer conditions
k_D	rate constant for deactivation, $m^3/(kg \cdot s)$
k_{mL}	mass transfer coefficient, m/s
k_P	apparent first-order reaction rate constant, $m^3/(kg \cdot s)$
k_R	intrinsic first-order rate constant, m/s
M, N	dimensions of position and time vectors, respectively
n	constant in Eq. (11) related to different mass transfer conditions
Q	volumetric superficial velocity, m^3/s
Re	Reynolds number ($=d_p G/\eta$)
r_A	H_2O_2 consumption rate, kg/(kg·s)
r_m	mass transfer rate, kg/(kg s)
Sc	Schmidt number ($=\eta/\rho D_f$)
St_D	Stanton number for mass transfer ($=k_{mL}\rho/G$)
t	time, s
U	superficial velocity averaged over the entire cross section of the bed, m/s
W	amount of immobilized Terminox Ultra catalase, kg
Y	dependent variable ($=a_m k_P^{-1} - k_R^{-1}$), s/m

Greek symbols

α	conversion at the reactor outlet ($=1-C_{A,Out}/C_{A,In}$) calculated from Eq. (16)
β_i	dimensionless coefficients expressed by Eq. (18) ($i=1$) and Eq. (19) ($i=2$)
ε	porosity
η	fluid viscosity, kg/(m·s)
ρ	fluid density, kg/m^3
ρ_U	bulk density, kg/m^3
τ	dimensionless time ($=tQ\rho_U/W$)

Subscripts

In	inlet
Out	outlet

REFERENCES

Alptekin Ö., Seyhan Tükel S., Yildirim D., Alagöz D., 2011. Covalent immobilization of catalase onto spacer-arm attached modified florisil: Characterization and application to batch and plug-flow type reactor systems. *Enzyme Microb. Technol*., 49, 547-554. DOI: 10.1016/j.enzmictec.2011.09.002.

Altomare R. E., Kohler J., Greenfield P. F., Kittrell J. R., 1974. Deactivation of immobilized beef liver catalase by hydrogen peroxide. *Biotechnol. Bioeng.*, 16, 1659-1673. DOI: 10.1002/bit.260161208.

Betancor L., Hidalgo A., Fernández-Lorente G., Mateo C., Fernández-Lafuente R., Guisan J. M., 2003. Preparation of a stable biocatalyst of bovine liver catalase using immobilization and postimmobilization techniques. *Biotechnol. Progres*, 19, 763-767. DOI: 10.1021/bp025785m.

Burghardt A., Bartelmus G. (Eds.), 2001. Models of Heterogeneous Fixed-Bed Catalitic Reactors, In: *Chemical Reactors Engineering. Part II. Heterogeneous Reactors*. Scientific Publishing Company, Warsaw, 170-277.

Costa S. A., Tzanov T., Carneiro F., Gubitz G. M., Cavaco-Paulo A., 2002a. Recycling of textile bleaching effluents for dyeing using immobilized catalase. *Biotechnol. Lett.*, 24, 173-176. DOI: 10.1023/a:1014136703369.

Costa S. A., Tzanov T., Filipa Carneiro A., Paar A., Gübitz G. M., Cavaco-Paulo A., 2002b. Studies of stabilization of native catalase using additives. *Enzyme Microb. Technol.*, 30, 387-391. DOI: 10.1016/S0141-0229(01)00505-1.

Curcio S., Ricca E., Saraceno A., Iorio G., Calabrò V., 2015. A mass transport/kinetic model for the description of inulin hydrolysis by immobilized inulinase. *J. Chem. Technol. Biotechnol.*, 90, 1782-1792. DOI: 10.1002/jctb.4485.

Deluca D. C., Dennis R., Smith W. G., 1995. Inactivation of an animal and a fungal catalase by hydrogen peroxide. *Arch. Biochem. Biophys.*, 320, 129-134. DOI: 10.1006/abbi.1995.1350.

Dizge N., Tansel B., 2010. External mass transfer analysis for simultaneous removal of carbohydrate and protein by immobilized activated sludge culture in a packed bed batch bioreactor. *J. Hazard. Mater.*, 184, 671-677. DOI: 10.1016/j.jhazmat.2010.08.090.

Eberhardt A. M., Pedroni V., Volpe M., Ferreira M. L., 2004. Immobilization of catalase from Aspergillus niger on inorganic and biopolymeric supports for H2O2 decomposition. *Appl. Catal. B: Environ.*, 47, 153-163. DOI: 10.1016/j.apcatb.2003.08.007.

Farkye N. Y., 2004. Cheese technology. *Int. J. Dairy Technol.*, 57, 91-98. DOI: 10.1111/j.1471-0307.2004.00146.x.

Fernández-Lafuente R., Rodriguez V., Guisán J. M., 1998. The coimmobilization of d-amino acid oxidase and catalase enables the quantitative transformation of d-amino acids (d-phenylalanine) into α-keto acids (phenylpyruvic acid). *Enzyme Microb. Technol.*, 23, 28-33. DOI: 10.1016/S0141-0229(98)00028-3.

Greenfield P. F., Kinzler D. D., Laurence R. L., 1975. Film diffusion and Michaelis-Menten kinetics in a packed-bed reactor. *Biotechnol. Bioeng.*, 17, 1555-1559. DOI: 10.1002/bit.260171014.

Illanes A., Wilson L., Vera C. (Eds.), 2014. Enzyme kinetics in a heterogeneous system, In: *Problem solving in enzyme biocatalysis*. John Wiley and Sons Ltd., Chichester, United Kingdom, 87-140.

Kalaga D. V., Dhar A., Dalvi S. V., Joshi J. B., 2014. Particle-liquid mass transfer in solid–liquid fluidized beds. *Chem. Eng. J.*, 245, 323-341. DOI: 10.1002/bit.260171014.

Mudliar S., Banerjee S., Vaidya A., Devotta S., 2008. Steady state model for evaluation of external and internal mass transfer effects in an immobilized biofilm. *Bioresource Technol.*, 99, 3468-3474. DOI: 10.1016/j.biortech.2007.08.001.

Rovito B. J., Kittrell J. R., 1973. Film and pore diffusion studies with immobilized glucose oxidase. *Biotechnol. Bioeng.*, 15, 143-161. DOI: 10.1002/bit.260150111.

Schoevaart R., Kieboom T., 2001. Combined catalytic reactions—Nature's way. *Chemical Innovation*, 31(12), 33-39.

Tarhan L., Telefoncu A., 1990. Characterization of immobilized glucose oxidase—catalase and their deactivation in a fluid-bed reactor. *Appl. Biochem. Biotechnol.*, 26, 45-57. DOI: 10.1007/BF02798392.

Tarhan L., Uslan A. H., 1990. Characterization and operational stability of immobilized catalase. *Process Biochem.*, 25(1), 14-18.

Tarhan L., 1995. Use of immobilised catalase to remove H_2O_2 used in the sterilisation of milk. *Process Biochem.*, 30, 623-628. DOI: 10.1016/0032-9592(94)00066-2.

Traher A. D., Kittrell J. R., 1974. Film diffusion studies of immobilized catalase in tubular flow reactors. *Biotechnol. Bioeng.*, 16, 419-422. DOI: 10.1002/bit.260160311.

USP Technologies Company, http://www.h2o2.com/, April 24, 2017.

Vasudevan P. T., Weiland R. H., 1990. Deactivation of catalase by hydrogen peroxide. *Biotechnol. Bioeng.*, 36, 783-789. DOI: 10.1002/bit.260360805.

Vasudeven P. T., Weiland R. H., 1993. Immobilized catalase: Deactivation and reactor stability. *Biotechnol. Bioeng.*, 41, 231-236. DOI: 10.1002/bit.260410209.

Vera-Avila L. E., Morales-Zamudio E., Garcia-Camacho M. P., 2004. Activity and reusability of sol-gel encapsulated α-amylase and catalase. Performance in flow-through systems. *J. Sol-Gel Sci. Technol.*, 30, 197-204. DOI: 10.1023/B:JSST.0000039505.49588.5d.

Zámocký M., Koller F., 1999. Understanding the structure and function of catalases: clues from molecular evolution and in vitro mutagenesis. *Prog. Biophys. Mol. Biol.*, 72, 19-66. DOI: 10.1016/S0079-6107(98)00058-3.

Received 10 October 2016
Received in revised form 9 May 2017
Accepted 23 May 2017